

# Eastern Arctic soundscape measured with a drifting vertical line array

Emma Reeves,<sup>1, a)</sup> Peter Gerstoft,<sup>1</sup> Peter Worcester,<sup>1</sup> and Matthew Dzieciuch<sup>1</sup>  
*Scripps Institution of Oceanography, University of California San Diego, La Jolla,  
 California 92093-0238*

(Dated: 3 September 2022)

The soundscape in the eastern Arctic was studied from April to September 2013 using a 22 element vertical hydrophone array as it drifted from near the North Pole (89°23'N, 62°35'W) to north of Fram Strait (83°45'N 4°28' W). The hydrophones recorded for 108 minutes on six days per week with a sampling rate of 1953.125 Hz. After removal of data corrupted by nonacoustic flow-related noise, 19 days throughout the transit period were analyzed. Major contributors include broadband and tonal ice noises, seismic airgun surveys, and earthquake *T* phases. Statistical spectral analyses show a broad peak at about 15 Hz similar to that previously observed and a mid-frequency decrease at  $f^{-2}$ . The median noise levels reflect a change in dominant sources, with ice noises (200–500 Hz) decreasing and seismic airgun surveys (10–50 Hz) increasing as the array transited southward. The median noise levels were among the lowest of the sparse reported observations in the eastern Arctic, but comparable to the more numerous observations of western Arctic noise levels.

## I. INTRODUCTION

The Arctic Ocean soundscape is defined by its sea ice cover. Internal frictional shearing, thermal stress fracturing, and interaction within leads generate distinct sounds that can exceed 100 dB re  $1\mu\text{ Pa}^2\text{ Hz}^{-1}$ . At the same time, the upward-refracting sound speed profile and nearly year-round ice cover create a propagation channel that preserves low frequency signals while attenuating higher frequency components. This unique environment depends strongly on the properties of the Arctic sea ice, including percentage of areal cover, thickness (age), and lateral extent. In the past decade, the Arctic sea ice has dramatically reduced in thickness as well as annual extent,<sup>1</sup> resulting in unknown changes to the soundscape.

Sea ice noise and the Arctic soundscape properties have historically been an area of interest in underwater acoustics.<sup>2,3</sup> Measurements of ice noises have shown that they are highly non-Gaussian,<sup>4</sup> varying in characteristic by the generating mechanism,<sup>5</sup> but often more prevalent near ice ridges.<sup>6,7</sup> The cumulative ambient noise levels generated by ice noise have been shown to correlate with environmental variables like wind, air pressure, and temperature.<sup>8,9,10,11</sup> Near the Marginal Ice Zone (MIZ), where the ice is subject to increased wave forcing, noise levels have been shown to increase as much as 10 dB from those further under the ice cap.<sup>12,13</sup> It is well known that the sea ice is a strong scatterer that attenuates high frequencies at a much higher rate than the open ocean,<sup>14</sup> although the exact attenuation coefficients depend on the local sea ice structure and have yet to be determined.<sup>15</sup> Due in large part to biological activity and experimental accessibility, the Western Arctic soundscape near the Beaufort Sea<sup>11,16,17,18</sup> has been studied more extensively than the eastern Arctic soundscape near and north of the Fram Strait. Studies north of 85°N are extremely rare.

In April 2013, a bottom-moored vertical hydrophone array was deployed at Ice Camp Barneo near 89°N, 62°W. The experiment was designed to study the propagation properties and transmission loss under the sea ice, as well as the northern polar soundscape. Around April 15, 2013 the mooring cable failed. The subsurface float rose to the surface where it remained constrained by the sea ice, with the array hanging below. It drifted southward with the Transpolar Current toward the Fram Strait, recording ambient noise as scheduled. MicroCAT pressure measurements (see Sec. II B) showed that the array was vertical under its own weight during much of the transit. The resulting data record the spatiotemporal variation of the far northern Arctic soundscape ( $> 85^\circ\text{N}$ ). In this study, the dataset is analyzed and the observations are interpreted in terms of previous studies of the Arctic soundscape.

The paper is organized as follows. In Sec. II, the acoustic experiment is described, data processing methods are explained, and collection of supplementary environmental data is discussed. In Sec. III, select noise events are discussed. In Sec. IV, the results of statistical soundscape analyses in both time and depth are presented. In the final Sec. V, Arctic soundscape power estimates from previous studies are compared with summer 2013. The goal of this paper is to establish an understanding of soundscape contributors and sound levels in the north-eastern Arctic during summer 2013.

## II. METHODS

### A. Acoustic measurements

A 600 m long bottom-moored acoustic receiving array was deployed at Ice Camp Barneo, 89°23.379'N, 62°35.159'W, on April 14, 2013. Twenty-two omnidirectional hydrophones were spaced along the array, with phones 1–10 separated by 14.5 m and phones 11–22 separated by logarithmically increasing spacing starting at

<sup>a)</sup>Corresponding author. Email: [ecreeves@ucsd.edu](mailto:ecreeves@ucsd.edu)

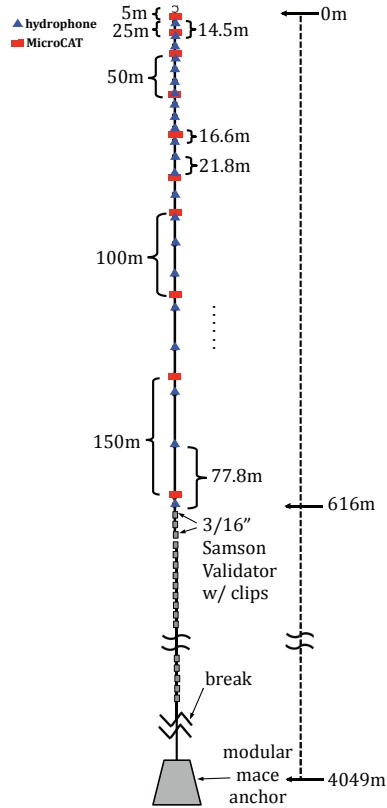


FIG. 1. A diagram of the array.

TABLE I. Array instrument spacing.

Hydrophone #	Hydrophone Depths (m)	MicroCAT Depths (m)	MicroCAT #
1	12	5	1
2	26.5	25	2
3	41	-	-
4	55.5	50	3
5	70	-	-
6	84.5	-	-
7	99	100	4
8	113.5	-	-
9	128	-	-
10	142.5	-	-
11	159.1	150	5
12	178.1	-	-
13	199.9	201	6
14	224.8	-	-
15	253.4	250	7
16	286.1	-	-
17	323.6	-	-
18	366.5	350	8
19	415.6	-	-
20	471.8	450	9
21	536.2	-	-
22	610	600	10

16.5 m (Table I, Fig. 1). The topmost hydrophone was located 12 m below the subsurface float. The hydrophones recorded underwater sound for 108 minutes six days per week (Sunday through Friday), starting at 1200 UTC, with a sampling frequency of 1,953.125 Hz. Acoustic recordings are available for 119 days between April 29 and September 20, 2013.

The raw acoustic recordings were scaled to be in units of instantaneous sound pressure using the analog-to-digital conversion parameters, the gain, and the hydrophone receiving sensitivity given by the manufacturer. The system noise floor was taken from a model combining the known self-noise of its individual components. The system was also tested in a Faraday cage and by calculating the coherence between multiple sensors recording noise in a quiet room, which both fit well with the modeled system noise floor.

Median spectral estimates were created by segmenting data across a given time period into 4096-point windows ( $\sim 2$  s), taking a 16,384-point Fast Fourier Transform of each window, and calculating the median of the individual spectral estimates. The frequency bins are 0.12 Hz for these estimates. Spectrograms were estimated separately using 512-point windowed segments ( $\sim 0.25$  s) zero-padded to 2048 points ( $df \approx 1$  Hz). All data were recorded at 84.5 m (hydrophone # 6) unless otherwise noted.

## B. MicroCATs

Ten Sea-Bird SBE 37-SM/SMP MicroCAT instruments were co-located with the hydrophones, spaced 25, 50, 50, 50, 50, 100, 100, and 150 m apart. The topmost MicroCAT was located 5 m below the subsurface float (Table I, Fig. 1). The MicroCATs began recording on April 28 and sampled continuously until September 19. The sampling period of the top four instruments was 480 s, the next five 380 s, and the deepest 300 s.

## C. GPS coordinates

A Xeos Technologies Kilo Iridium-GPS mooring location beacon located on top of the subsurface float began transmitting ALARM messages on May 3, 2013, indicating that the mooring had prematurely surfaced. The reported position at the time of surfacing was  $88^{\circ}50.30'N$ ,  $51^{\circ}17.91'W$ , 63 km from the deployment location. Analysis of an acoustic survey on April 14, following deployment of the mooring, revealed that the acoustic release was significantly shallower than expected. The implication is that the mooring failed shortly after deployment, but the subsurface float was trapped beneath sea ice, preventing the location beacon from obtaining GPS positions or transmitting ALARM messages until it was exposed on May 3. The float drifted southward in the Transpolar Drift. There were frequent gaps in transmis-

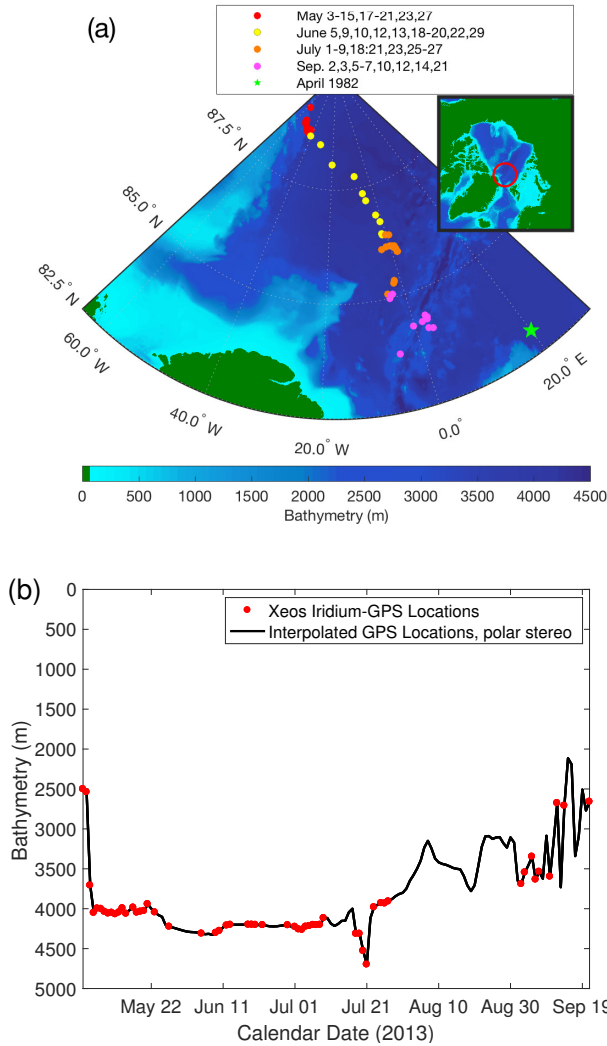


FIG. 2. (Color online) (a) A Bathymetric relief map showing the location of the receiving array by month and the location of the April 1982 FRAM IV ice camp (star). (b) Bathymetry at the receiving array location along its drift path, from May 3 to September 21, 2013.

sions from the location beacon, which are presumed to coincide with periods when the subsurface float was covered by sea ice (Fig. 2(a)). The buoy was recovered on September 21, 2013, at  $84^{\circ}03.50'N$ ,  $003^{\circ}05.83'W$  (Fig. 3). The mooring line was found to have parted immediately above the anchor (Fig. 1).

#### D. Bathymetry

A 56-day discontinuous timeseries of the bathymetry along the array drift path between May 3 and September 21 was created using the International Bathymetric Chart of the Arctic Ocean from the National Centers for Environmental Information (Fig. 2(b)). The georeferenced polar stereo projection bathymetry grid was in-



FIG. 3. (Color online) Recovery of the array near Svalbard  $84^{\circ}03.50'N$ ,  $03^{\circ}05.83'W$  on September 21, 2013 (Credit: Hanne Sagen, Nansen Center in Bergen, Norway).

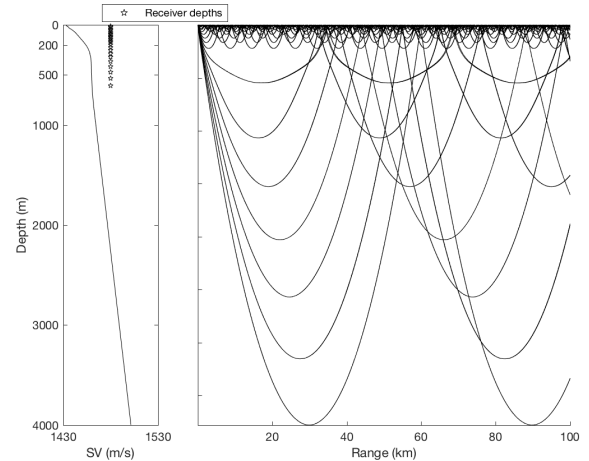


FIG. 4. A Bellhop ray propagation model<sup>19</sup> for the sound speed profile measured at Ice Camp Barneo. The sound speed profile was measured to 1000 m depth and linearly extrapolated to 4000 m. Thirty-five rays were launched with angles between  $\pm 17^{\circ}$  from horizontal. The surface duct at 0–200 m depth is characteristic Arctic acoustic propagation.

dexed at the desired coordinate locations to obtain the timeseries data. Acoustic propagation along the drift path is ray-dominated and confined primarily to the top 200 m, so the variation in bathymetry has a minimal effect on the measured ambient noise (Fig. 4).

#### E. Filtering/Noise Removal

Low frequency ( $f < 10$  Hz) cable strum was observed but kept in the spectral estimates for comparison purposes.

Strong spectral bands were also observed, exceeding  $100$  dB re  $1 \mu\text{Pa}^2 \text{Hz}^{-1}$  and extending to the Nyquist frequency ( $976.56$  Hz) (Fig. 5). Periods of unexpectedly low pressures (depth) on the MicroCATs corresponded to the periods of high acoustic power (Fig. 6(a)). It therefore seems unlikely that these high spectral levels are due to propagating acoustic noise. With the buoyant subsurface float constrained to the surface, flow past the

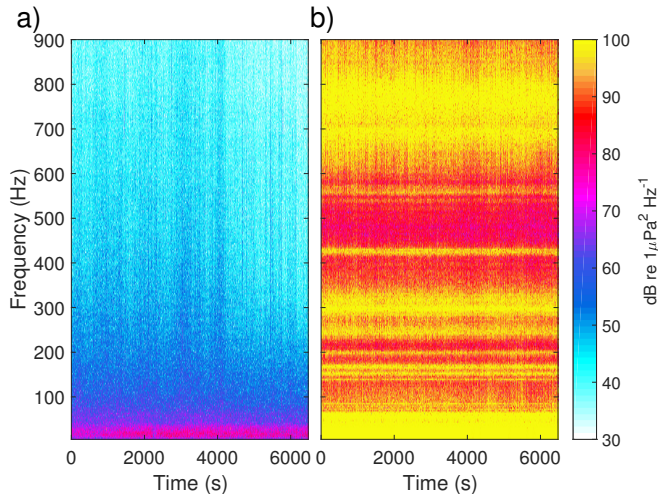


FIG. 5. (Color online) Spectrograms of post-processed received hydrophone pressures for (a) a good recording of the Arctic soundscape, with the highest power levels focused at  $f < 100$  Hz, and (b) a bad recording affected by flow-related noise, with strong multi-tonal bands in the frequency domain.

mooring lifts and thus tilts the array and reduces the MicroCAT pressures (depths). Potential non-acoustic noise sources associated with flow past the mooring include strumming, flow noise, and/or mechanical vibrations.

To remove data affected by flow noise, the median MicroCAT pressure for each day was computed. The pressure on the deepest MicroCAT (600 m) had the largest variation between days and was used as an indicator of flow-related noise (Fig. 6(b)). By comparing the good and bad spectrograms (Fig. 5) with their median MicroCAT pressures, it was found that most corrupted data had a median pressure level below 604.9 dBars. Therefore days with  $p_{\text{MicroCAT}} < 604.9$  dBars were not used. This method selected 19 days for further analysis: April 30, May 1, 2, 7, 8, 9, 12, 14, June 16, 18, July 3, 14, 19, 24, August 2, and September 10, 18, 19, 20.

### III. SOUNDSCAPE CONTRIBUTORS

The near-polar Arctic under-ice soundscape is generated by sea ice, wind, anthropogenic and biologic noise sources that travel long distances within the subsurface propagation duct. The following section discusses specific examples of underwater noise for the eastern Arctic soundscape of summer 2013.

#### A. Background noise levels

The soundscape observed during the array transit consists primarily of background noise from distant events. The spectrum is characterized by a broad spectral peak at 10–20 Hz and a power fall-off above  $\sim 100$

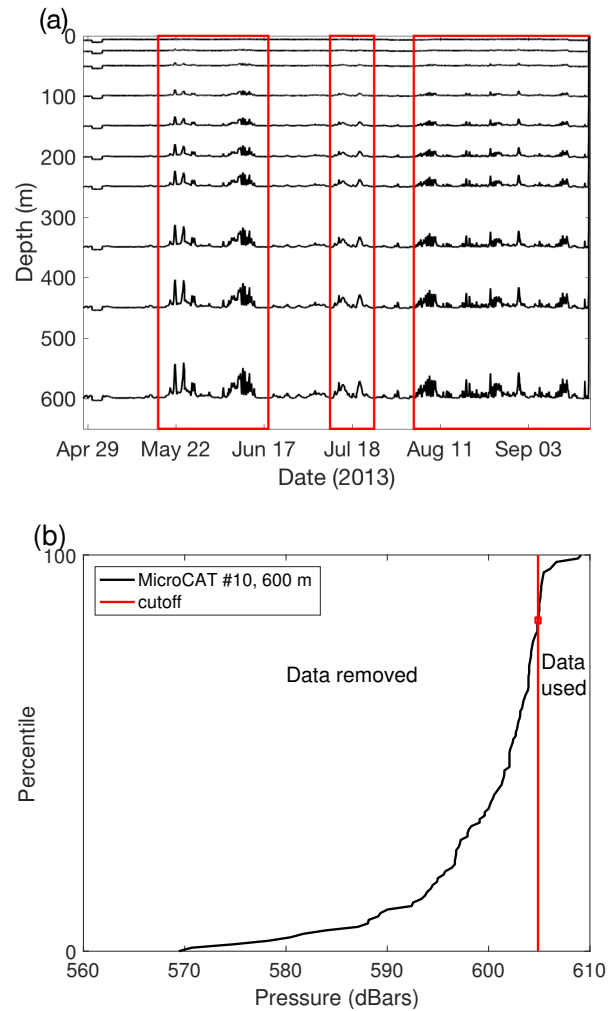


FIG. 6. (Color online) MicroCAT pressure measurements for (a) the 145-day timeseries at all 10 depths, starting April 28, and (b) the deepest MicroCAT (600 m), sorted by increasing pressure, together with the empirical depth cutoff (vertical line). The periods of MicroCAT shallowing (rectangles) correspond to periods of flow-related noise on the hydrophones.

Hz (Fig. 7(a), log-frequency). The hydrophone received pressure timeseries shows that the background noise and broadband noise vary by a factor of 10, despite appearing similar in spectrogram estimates (Fig. 7(a), 7(b)). The hydrophone timeseries also emphasizes the wide variability within a recording period due to ice noise (Fig. 7(b)). The median spectral estimate for each spectrogram can be compared to the daily and monthly median spectral estimates (Fig. 12), demonstrating the smoothing effect of using a longer recording for the median spectral estimate.

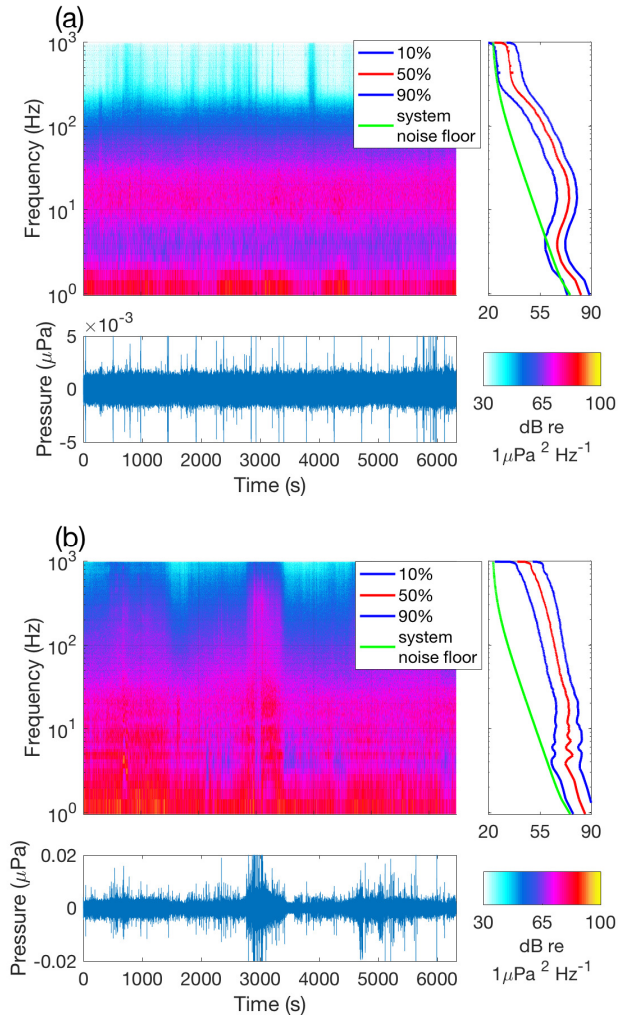


FIG. 7. (Color online) Spectrograms (log–frequency scale) of the Arctic soundscape for (a) hydrophone recording day May 14 and (b) hydrophone recording day May 8 containing broadband ice noise. The  $\sim 15$  Hz peak is due to multiple ice scattering and high–frequency attenuation. Pulses every 480 s in (a) were generated by the MicroCAT instrument pumps.

## B. Ice-generated noise

Ice noises were observed to be either broadband or tonal in nature, lasting from 1 to 100 s. Broadband ice noise extended across the frequency band (Fig. 7(b), log–frequency). Tonal ice noises are single–frequency or harmonic signatures modulated in time (Figs. 8(a)–8(c), linear frequency).

Xie and Farmer<sup>20</sup> demonstrated that constant–frequency ice tonals could be modeled as resonance in an infinitely long sea ice block of uniform height, density, and velocity generated by frictional shear stress on its edge. The nonlinear tonals observed here may indicate anomalies in the local height or composition of the sea ice or a frictional stress that is velocity–dependent (Fig. 8(a)). The degree of nonlinearity varies between

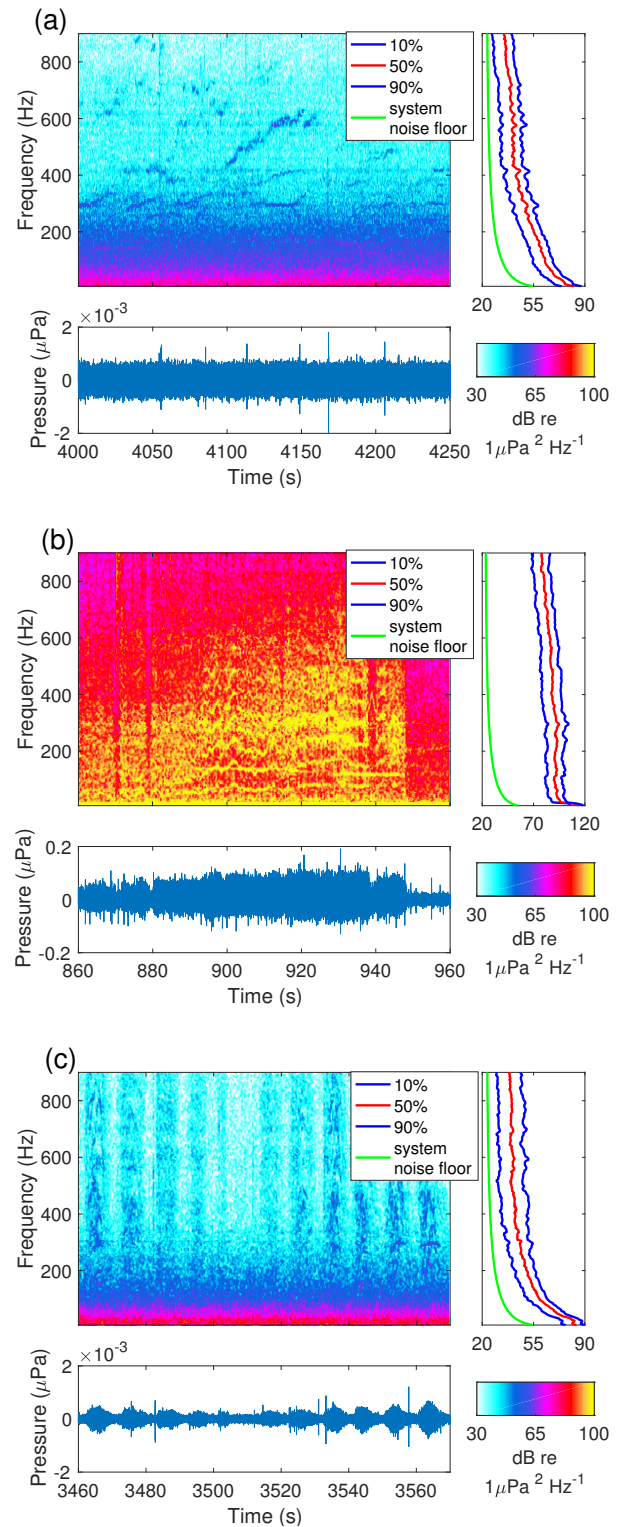


FIG. 8. (Color online) Spectrograms (linear–frequency scale) of ice tonal noises (a) without harmonics, recorded on May 2, (b) with near-constant harmonic tonals, recorded on April 30, and (c) modulated by ocean swell, recorded on September 18, 230 km from the sea ice edge.

hydrophone recordings (Fig. 8(b)), indicating that significant changes in ice properties and dynamics may occur within the spatiotemporal span of 2–3 array drift days.

Another interesting case is ocean swell–modulated ice tonals, with period  $\sim 9$  s (Fig. 8(c)). Ocean waves impinging on the sea ice edge can generate seismic or flexural waves that propagate within the sea ice, if the frequency–ice product is less than about 300 Hz–m.<sup>21</sup> Swell–modulated ice tonals observed on the receiving array suggest that these effects can be seen as far as 230 km from the ice edge.

### C. Seismic Survey Signals

Broadband pressure pulses generated by airguns are used to image the ocean bottom subsurface during seismic surveys. At long distances, higher frequencies ( $f > 100$  Hz) are attenuated by scattering at the water–ice boundary. The resulting pulses can be observed on hydrophone receivers at  $f < 50$  Hz. Distant noise from seismic surveys can be observed almost daily in the Fram Strait during summer months. For example, airgun surveys were observed on 90–95% of days between July and September 2009.<sup>22</sup>

Airgun survey pulses were observed on 11 out of 19 selected recording days between May 7 and Sep. 19 (Fig. 9(a), linear frequency). Due to irregular sampling, the 1–3 seismic surveys recorded per month represented seismic surveys on 43%–100% of the recording days in May through September. These pulses arrived at about  $\pm 4^\circ$  from horizontal (Fig. 9(b)), as determined by incoherently averaged 2.1 s Bartlett beamformer estimates across June 16. For other recording days, the pulse arrivals ranged between  $5$ – $15^\circ$ . The shallow arrival angles indicate that these low–frequency signals travel great distances within the subsurface sound propagation channel.

Location, type and date of surveys in Norwegian territory are available through the Norwegian Petroleum Directorate. According to these data, the array was between 1800 and 3500 km distant from seismic surveys at the beginning of its transit in April and 1000 to 3000 km at the end in September. Using the Advanced Microwave Scanning Radiometer-2 (AMSR-2) 89-GHz channel satellite dataset (Appendix),<sup>23</sup> the array was found to be about 1000 km distant from the ice edge in April and 200 km distant in September (Fig. 10). It is likely that the signals observed arrived from the closest surveys. Thus airgun signals received at 70–80 dB re  $1 \mu\text{Pa}^2 \text{Hz}^{-1}$  had propagated approximately 800 km in open water and anywhere from 200 to 1000 km under the ice.

### D. Arctic Basin Earthquakes

Frequent seismic activity and low–magnitude earthquakes occur where the North American/Eurasian plate

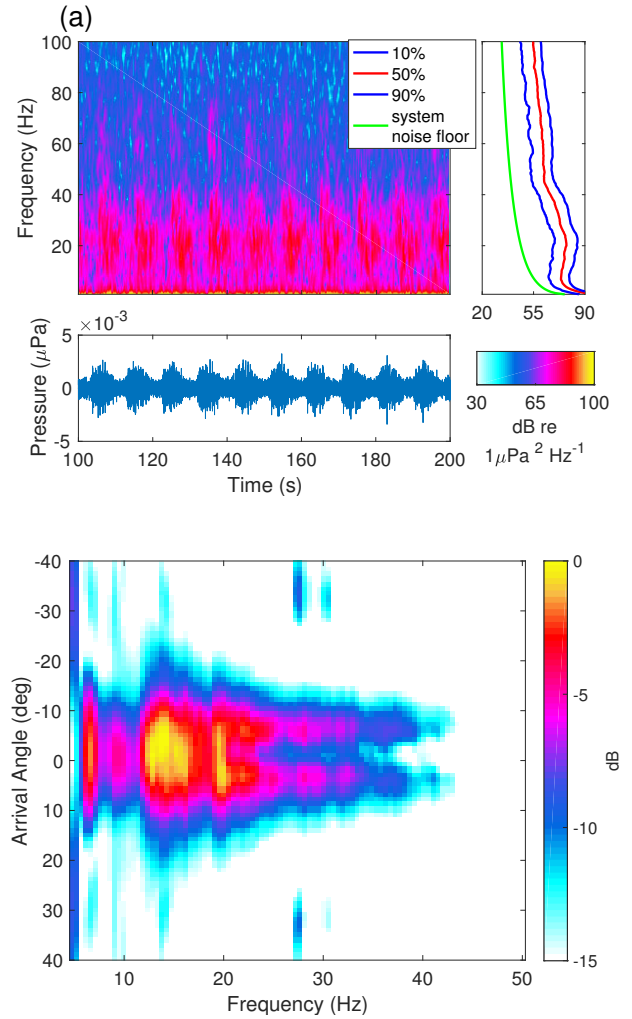


FIG. 9. (Color online) (a) Spectrogram of low–frequency pulses generated by a distant airgun survey, recorded on June 16. The received hydrophone pressure was bandpass filtered 15–80 Hz. (b) Normalized averaged Bartlett beamformer at 5–50 Hz for June 16. Noise arrives from  $\pm 4^\circ$ .

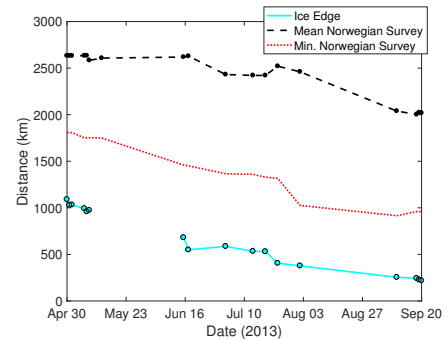


FIG. 10. (Color online) Distance from the array to the ice edge, found using AMSR2 data, and to seismic surveys in the Norwegian Polar Directorate database for the 19 selected days. The minimum and mean distances were calculated using all Norwegian seismic surveys within the database during May–September, 2013.

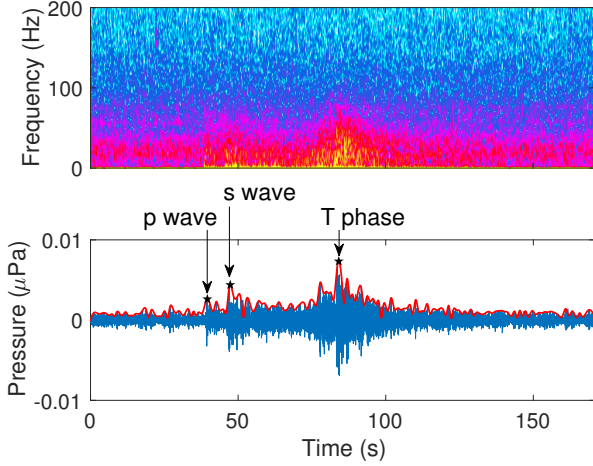


FIG. 11. (Color online) Spectrogram and received hydrophone pressure ( $\mu\text{Pa}$ ) of an earthquake on August 2.

boundary meets the Gakkel Ridge. Because the nearest seismic stations are land-based and up to 1000 km away, many of these earthquakes are not registered with the Global Seismic Network. A receiving array deployed in the Lincoln Sea has been successful in detecting and locating earthquakes originating from this juncture.<sup>24</sup>

Earthquakes can be observed acoustically through the  $T$  phase arrival. The  $T$  phase is an acoustic pressure wave coupled into the water column from the ocean bottom at an anomaly (for example, a seamount). The  $T$  phase arrives after the  $P$  and  $S$  seismic arrivals but is the most visible arrival. The differences in arrival time between the three waves can be used to localize the earthquake if appropriate propagation velocities are known.  $T$  phase arrivals were observed during the array transit in summer 2013, indicating that Arctic basin earthquakes also contribute to the low-frequency soundscape (Fig. 11). The earthquake center was estimated to be about 100 km from the receiving array.

## IV. RESULTS

### A. Eastern Arctic soundscape, summer 2013

In this section, spectral estimates from different months at several depths are compared to establish the spatiotemporal dependence of ambient noise in the eastern Arctic during summer 2013.

Three days were selected to examine the daily variation in median ambient noise levels: May 7, July 14, September 10 (Fig. 12). The 10<sup>th</sup>, 50<sup>th</sup> (median), and 90<sup>th</sup> percentiles for May 2013 show the variation in spectral shape between the most and least frequent generation mechanisms. For example, cable strum is visible at  $f < 10$  Hz in the 90<sup>th</sup> percentile. Other peaks near 10–100 Hz may be caused by flow-related noise or seismic survey

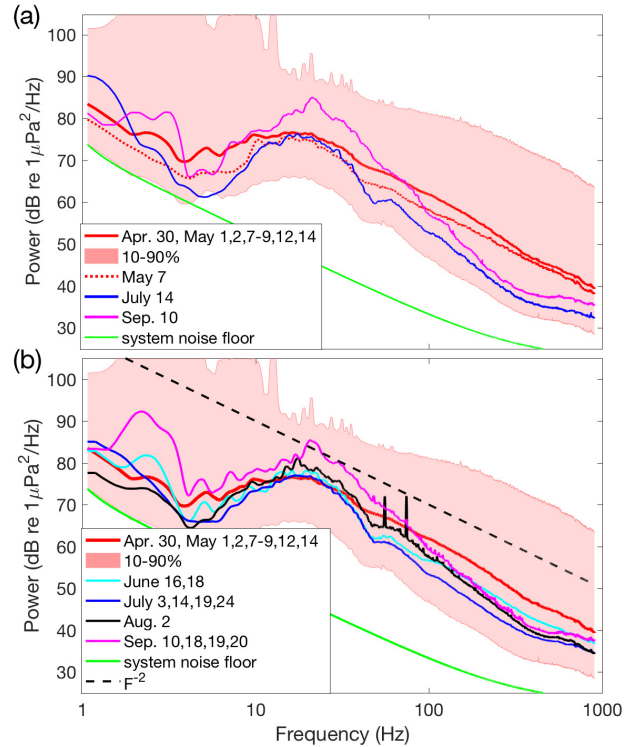


FIG. 12. (Color online) Median (50%), 10%, and 90% spectral estimates for May are compared with (a) daily estimates for May 7, July 14, and September 10, and (b) monthly estimates for June, July, August, and September in 2013.

activity. The 10<sup>th</sup> percentile is defined by single, broad peak at 15 Hz due to distant sources within the sound channel. The daily median estimates progress from least to most peaked, with May 7 showing a peak-to-peak (15 to 900 Hz) difference of 26 dB and September 10 showing a peak-to-peak difference of 44 dB. This trend indicates that the earlier spatiotemporal recordings contain more higher frequency noises whereas the later recordings were influenced by lower frequency sources.

The trend of increasing peakedness in the median spectral is more apparent in the monthly median spectra (Fig. 12). At low frequencies ( $f < 100$  Hz), an increase in median ambient noise levels corresponds to decreasing distance to the ice edge and to seismic survey activity. At higher frequencies ( $f > 100$  Hz) median ambient noise levels decrease with time, corresponding to fewer ice creak signatures observed in spectrograms. When limited data was available, such as in August, the median monthly spectra was likely to show evidence of flow-related noise i.e. at about 75 and 90 Hz, despite efforts to remove this noise.

It is interesting to note these spatiotemporal differences in median ambient noise levels with proximity to the Marginal Ice Zone (MIZ); the effect of the MIZ on ambient noise was previously studied only for distances less than 150 km<sup>12</sup>. The decrease in high-frequency median ambient noise levels may represent a physical change

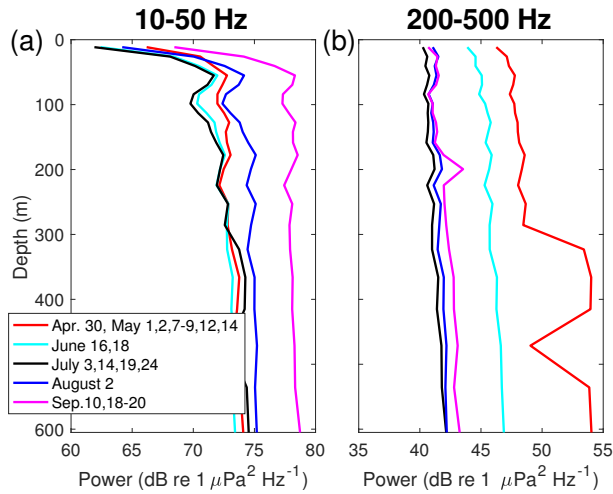


FIG. 13. (Color online) Depth-dependence of eastern Arctic median monthly ambient noise power, averaged across (a) 10–50 Hz and (b) 200–500 Hz to represent high- and low-frequency phenomena. In both cases, the system noise floor is below the range shown.

in the spatial or temporal ice stress field.

The median ambient noise depth profile during summer 2013 was found to depend on frequency. At low frequencies (10–50 Hz), a local peak in median ambient noise is centered in the subsurface propagation channel at the depth where ice reflections and upward refracting rays converge (Fig. 13). Below the sound channel and at higher frequencies (200–500 Hz), the median noise level is constant with depth as expected for an isotropic distribution of surface sources (Fig. 13). There is a strong signal during May at about 400 – 600 m depth that is likely due to flow-related noise, which could not be completely removed from the lower hydrophones using the noise filtering method (Sec. II E).

## B. Comparison of Arctic soundscapes

The summer 2013 median ambient noise results are here compared with historical estimates from both western and eastern Arctic stations. The median spectral estimates for May 2013 was below, but similarly structured to, a composite spectral estimate from April 1982.<sup>9</sup> The peak at 15 Hz appears less prominent at lower frequencies in 2013 than in 1982. In comparison, a spectral estimate recorded in the Beaufort Sea in April 1975 shows comparable ambient noise levels and structure to 2013 but does not extend to lower frequencies (Fig. 14).<sup>7</sup> The differences in these spectra may be caused by environmental factors or by experimental factors, including recording length and post-processing methods, which were not published alongside the results.

The broad peak at 15 Hz in all estimates can be attributed to distant ice and seismic survey noises propa-

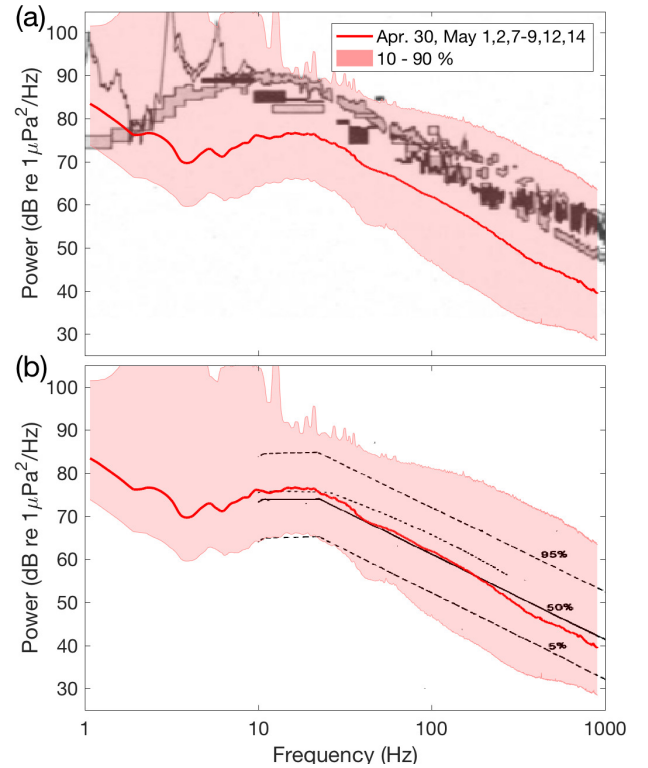


FIG. 14. (Color online) Median spectral estimate for May 2013, at 84.5 m depth, have power levels below (a) the April 1982 FRAM IV estimate,<sup>9</sup> at 99 m depth, but are about equal to (b) the April 1975 Polar Research Laboratory estimate from the Beaufort Sea (see Table II).<sup>7</sup>

gating in the sound channel,<sup>9</sup> as higher frequencies are more attenuated and lower frequencies have long wavelengths compared to the channel. The higher frequencies fall off at a consistent rate of  $f^{-2}$ . It is likely that an increased cumulative ice noise source level increases high frequency noise, thus reducing the fall off rate (Fig. 12).

Fig. 15 demonstrates the wide variability in Arctic ambient noise estimates across frequency, year, and study. This variability arises from a complex relationship between the Arctic soundscape and both environmental and anthropogenic factors, such as sea ice percent cover, sea ice age/thickness, barometric conditions and wind patterns, local subsurface currents, seismic survey activity, and marine biologic activity. The studies shown indicate that, without correction for environmental factors, there is not a significant trend in the Arctic soundscape power levels between 1960 and 2013, but that frequency-dependent ambient noise levels are within a 30–40 dB range for both regions of the ice covered Arctic.

## V. CONCLUSIONS

Between April and September, 2013, a 22-element vertical hydrophone array recorded the eastern Arctic

TABLE II. Soundscape noise level estimates in the Arctic Ocean.

	Location (lat, lon)	Experiment	Dates	15 Hz	50 Hz	100 Hz	500 Hz	1 kHz
<b>Eastern Arctic</b>	86°N 56.9°W – 89°N 1°E	May–June 2013	05/2013 – 06/2013	76.5	66	60.2	43.7	-
	86°N 1.3°E – 83.8°N 4.5°E	July–Sep. 2013	07/2013 – 09/2013	78.7	64.9	55.6	37.6	-
	83°N 20°E	FRAM IV <sup>9</sup>	04/1982	90	79.5	73	60	53
	82°N 168°E 75°N 168°W	Mellen, Marsh 1985 <sup>25</sup>	09–10/1961 05–09/1962	72 63	70 64	61 49	51 37	40 32
<b>Western Arctic</b>	78.5°N 105.25°W	Ice Pack I <sup>26</sup>	27/04/1961	50	42	38	37	20
			28/04/1961	58	52	51	52	51
	74.5°N 115.1°W Beaufort Sea	Ice Pack II <sup>26</sup> PRL <sup>27</sup>	9/2–3/1961	-	57	56	52	43
			April 1975	73	68	62	48	43
	~72°N 142°W	AIDJEX <sup>18</sup>	08/1975	65–85	65–75	-	-	38–55
			11/1975	70–90	65–88	-	-	40–70
			02/1976	65–90	60–90	-	-	35–70
			05/1976	65–88	60–90	-	-	37–68
	71°N 126.07°W	Kinda et al. 2013 <sup>11</sup>	11/2004 – 06/2005	68	69	66	58	54
	72.46°N 157.4°W	Roth et al. 2011 <sup>16</sup>	09/2008	84	80	74	60	56
03/2009			84	70	62	48	48	
05/2009			76	61	56	44	44	

for 108 minutes/day between 89°N, 62°W and Svalbard (north of the Fram Strait). The data were analyzed to produce spectral estimates of the median soundscape and demonstrate that ice noise and seismic airgun surveys were the dominant noise sources. The median ambient noise level for May 2013 was below a similar eastern Arctic estimate from April 1982,<sup>9</sup> but comparable to a western Arctic estimate from April 1975.<sup>7</sup> A multi-decadal summary of Arctic soundscape studies demonstrates that the estimated ambient noise levels depend strongly on experimental and environmental parameters and that there is not a significant trend in ambient noise levels among the studies examined.

## ACKNOWLEDGMENTS

We would like to thank John Colosi for providing the MicroCAT data, John Kemp and the WHOI Mooring Operations and Engineering Group for their assistance, and Hanne Sagen and the Norwegian Coast Guard for assistance in recovering the array mooring.

This work is supported by the Office of Naval Research under Award Numbers N00014-13-1-0632 and N00014-12-1-0226. Any opinions, findings, and conclusions or recommendations expressed in this publication are those of the authors and do not necessarily reflect the views of the Office of Naval Research.

## Appendix A

Daily sea ice concentration, defined as the areal percentage of satellite imagery above a certain brightness level, was obtained from the Advanced Microwave Scanning Radiometer-2 (AMSR-2) 89-GHz channel satellite dataset,<sup>23</sup> provided in a 4 km X 4 km gridded format from the Institute of Environmental Physics, University of Bremen, Germany (Fig. A.1). The sea ice concentration ranges from 0 (no ice) to 100 (solid ice). The georeferenced latitude and longitude grids were transformed into regular latitude and longitude grids with 0.1° resolution and the ice concentration was interpolated to the array location.

N-S and E-W wind velocity components were obtained from the European Center for Medium-Range Weather Forecasts (ECMWF) (Fig. A.1). The ERA-Interim reanalysis from which the data was drawn uses 30 minute time steps and a spectral T255 geographic resolution corresponding to 79 km spacing on a reduced Gaussian grid.<sup>28</sup> Local wind velocity for the 10 m isobar at the array location was extracted.

<sup>1</sup>R. Lindsay and A. Schweiger, “Arctic sea ice thickness loss determined using subsurface, aircraft, and satellite observations,” *T.C.* **9**, 269–283 (2015).

<sup>2</sup>I. Dyer, “The song of sea ice and other Arctic Ocean melodies,” in *Arctic Technology and Policy*, edited by I. Dyer and C. Chrysostomidis (Hemisphere, New York, 1984), pp. 11–37.

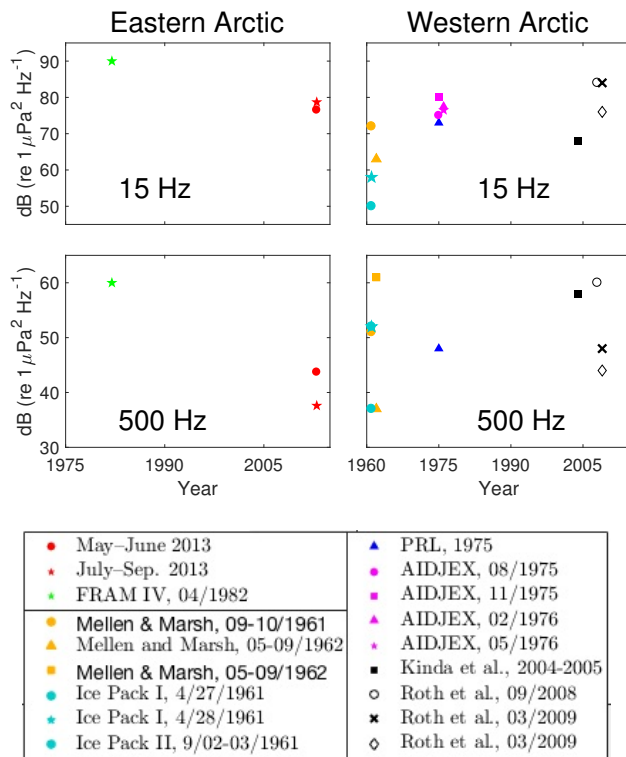


FIG. 15. (Color online) Scatter plot of median ambient noise level results for 15 Hz and 500 Hz from various studies in both the eastern and western Arctic (see Table II).

- <sup>3</sup>W. C. Cummings, O.I. Diachok, and J. D. Shaffer, “Acoustic Transients of the Marginal Sea Ice Zone: A Provisional Catalog,” *Naval Research Laboratory Memorandum Report 6408*, DTIC Number ADA214142. Naval Research Lab, Washington, D.C. (1989).
- <sup>4</sup>J.G. Veitch and A.R.Wilks, “A characterization of Arctic under-sea noise,” *J. Acoust. Soc. Am.* **77**, 989–999 (1985).
- <sup>5</sup>G.B. Kinda, Y. Simard, C. Gervaise, J.I. Mars, and L. Fortier, “Arctic underwater noise transients from sea ice deformation: Characteristics, annual time series, and forcing in Beaufort Sea,” *J. Acoust. Soc. Am.* **138**, 2034–2045 (2015).
- <sup>6</sup>O.I. Diachok, “Effects of sea ice ridges on sound propagation in the Arctic Ocean,” *J. Acoust. Soc. Am.* **59**, 1110–1120 (1976).
- <sup>7</sup>B.M. Buck and J.H. Wilson, “Nearfield noise measurements from an Arctic pressure ridge,” *J. Acoust. Soc. Am.* **80**, 256–264 (1986).
- <sup>8</sup>C.R. Greene and B.M. Buck, “Arctic Ocean Ambient Noise,” *J. Acoust. Soc. Am.* **36**, 1218 (1964).
- <sup>9</sup>N.C. Makris and I. Dyer, “Environmental correlates of pack ice noise,” *J. Acoust. Soc. Am.* **79**, 1434–1440 (1986).
- <sup>10</sup>N.C. Makris and I. Dyer, “Environmental correlates of Arctic ice-edge noise,” *J. Acoust. Soc. Am.* **90**, 3288–3298 (1991).
- <sup>11</sup>G.B. Kinda, Y. Simard, C. Gervaise, J.I. Mars, and L. Fortier, “Under-ice ambient noise in the Eastern Beaufort Sea, Canadian Arctic, and its relation to environmental forcing,” *J. Acoust. Soc. Am.* **134**, 77–87 (2013).
- <sup>12</sup>O.I. Diachok and R.S. Winokur, “Spatial variability of underwater ambient noise at the Arctic ice-water boundary,” *J. Acoust. Soc. Am.* **55**, 750–753 (1974).
- <sup>13</sup>F. Geyer, H. Sagen, G. Hope, M. Babiker, and P. F. Worcester, “Identification and quantification of soundscape components in the Marginal Ice Zone,” *J. Acoust. Soc. Am.* **139**, 1873–1885 (2016).

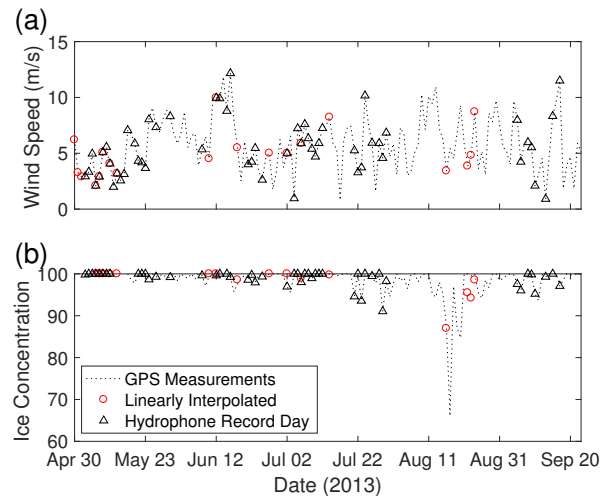


FIG. A.1. (a) Wind speed from the ERA-Interim model re-analysis at the 10 m isobar.<sup>28</sup> The wind components were extracted at the interpolated array location for the 12:00 UTC observation. (b) Sea ice concentration from pre-processed AMSR-II satellite imagery.<sup>23</sup> The concentration values were interpolated at the array locations from a  $0.5^\circ$ -resolution grid.

- <sup>14</sup>O. Diachok, “Arctic hydroacoustics,” *Cold Reg. Sci. Technol.* **2**, 186–201.
- <sup>15</sup>D. Tollefsen and H. Sagen, “Seismic exploration noise reduction in the Marginal Ice Zone,” *J. Acoust. Soc. Am.* **136**, EL47–52 (2014).
- <sup>16</sup>E. H. Roth, J. A. Hildebrand, S. M. Wiggins, and D. Ross, “Underwater ambient noise on the Chuckchi Sea continental slope from 2006-2009,” *J. Acoust. Soc. Am.* **131**, 104–110 (2012).
- <sup>17</sup>C. L. Berchok, P. J. Clapham, J. Crance, S. E. Moore, J. Napp, J. Overland, M. Wang, P. Stabeno, M. Guerra, and C. Clark, “Passive acoustic detection and monitoring of endangered whales in the Arctic (Beaufort, Chukchi) and Ecosystem observations in the Chukchi Sea: Biophysical moorings and climate modeling,” Annual Report 2012, contract M09PC00016 (AKC 083), Bureau of Ocean Energy Management, Regulation, and Enforcement, Anchorage, Alaska.
- <sup>18</sup>J. K. Lewis and W. W. Denner, “Arctic ambient noise in the Beaufort Sea: Seasonal space and time scales,” *J. Acoust. Soc. Am.* **82**, 988–997 (1987).
- <sup>19</sup>F.B. Jensen, W.A. Kuperman, M.B. Porter, and H. Schmidt, *Computational Ocean Acoustics* (Springer, New York, New York, 2011), pp. 27–28.
- <sup>20</sup>Y. Xie and D. M. Farmer, “The sound of ice break-up and floe interaction,” *J. Acoust. Soc. Am.* **91**, 2215–2231 (1992).
- <sup>21</sup>P.J. Stein, “Interpretation of a few ice event transients,” *J. Acoust. Soc. Am.* **83**, 617–622 (1988).
- <sup>22</sup>S.E. Moore, K.M. Stafford, H. Melling, C. Berchok, Ø. Wiig, K.M. Kovacs, C. Lydersen, and J. Richter-Menge, “Comparing marine mammal acoustic habitats in Atlantic and Pacific sectors of the High Arctic: year-long records from Fram Strait and the Chukchi Plateau,” *Polar Biol.* **35**, 475–480 (2012).
- <sup>23</sup>G. Spreen, L. Kaleschke, and G. Heygster “Sea ice remote sensing using AMSR-E 89 GHz channels,” *J. Geophys. Res.* **113**, C02S03 (2008).
- <sup>24</sup>R.A. Sohn and J.A. Hildebrand, “Hydroacoustic Earthquake Detection in the Arctic Basin with the Spinnaker Array,” *B. Seismol. Soc. Am.* **91**, 572–579 (2001).
- <sup>25</sup>R.H. Mellen and H.W. Marsh, “Underwater sound in the Arctic Ocean,” Accession Number AD718140. U.S. Navy Underwater Sound Laboratory, New London, Connecticut, 1965.
- <sup>26</sup>A.R. Milne and J.H. Ganton, “Ambient Noise under Arctic Sea

- Ice,” *J. Acoust. Soc. Am.* **36**, 855–863 (1964).
- <sup>27</sup>B. Buck, “Preliminary under-ice propagation models based on synoptic ice roughness,” *PRL TR-30* (May 1981). Seattle, Washington.
- <sup>28</sup>D.P. Dee, et al., “The ERA-Interim reanalysis: configuration and performance of the data assimilation system,” *Q. J. R. Meteorolog. Soc.* **137**, 1477–870X (2011).